

Effect of Surfaces on Amyloid Fibril Formation

Bradley Moores¹, Elizabeth Drolle², Simon J. Attwood¹, Janet Simons², Zoya Leonenko^{1,2*}

¹ Department of Physics and Astronomy, University of Waterloo, Waterloo, Ontario, Canada, ² Department of Biology, University of Waterloo, Waterloo, Ontario, Canada

Abstract

Using atomic force microscopy (AFM) we investigated the interaction of amyloid beta (A β) (1–42) peptide with chemically modified surfaces in order to better understand the mechanism of amyloid toxicity, which involves interaction of amyloid with cell membrane surfaces. We compared the structure and density of A β fibrils on positively and negatively charged as well as hydrophobic chemically-modified surfaces at physiologically relevant conditions. We report that due to the complex distribution of charge and hydrophobicity amyloid oligomers bind to all types of surfaces investigated (CH₃, COOH, and NH₂) although the charge and hydrophobicity of surfaces affected the structure and size of amyloid deposits as well as surface coverage. Hydrophobic surfaces promote formation of spherical amorphous clusters, while charged surfaces promote protofibril formation. We used the nonlinear Poisson-Boltzmann equation (PBE) approach to analyze the electrostatic interactions of amyloid monomers and oligomers with modified surfaces to complement our AFM data.

Citation: Moores B, Drolle E, Attwood SJ, Simons J, Leonenko Z (2011) Effect of Surfaces on Amyloid Fibril Formation. PLoS ONE 6(10): e25954. doi:10.1371/journal.pone.0025954

Editor: Igor Sokolov, Clarkson University, United States of America

Received: June 7, 2011; **Accepted:** September 14, 2011; **Published:** October 10, 2011

Copyright: © 2011 Moores et al. This is an open-access article distributed under the terms of the Creative Commons Attribution License, which permits unrestricted use, distribution, and reproduction in any medium, provided the original author and source are credited.

Funding: This work was supported by the Natural Science and Engineering Council of Canada (NSERC), <http://www.nserc-crsng.gc.ca>, Canada Foundation for Innovation, www.innovation.ca, and Ontario Ministry of Research and Innovation, www.mri.gov.on.ca: Ontario Research Fund (ORF), and Waterloo Institute for Nanotechnology (WIN), www.nano.uwaterloo.ca. JS is an undergraduate student supported by NSERC USRA award, BM is a MS student supported by NSERC Discovery grant (ZL) and WIN Graduate Fellowship (BM), ED is a PhD student supported by NSERC Graduate Scholarship (ED), Simon Attwood is a Postdoctoral Fellow supported by NSERC Discovery grant (ZL). The funders had no role in study design, data collection and analysis, decision to publish or preparation of the manuscript.

Competing Interests: The authors have declared that no competing interests exist.

* E-mail: zleonenk@uwaterloo.ca

Introduction

Amyloid fibrils are implicated in many neurodegenerative diseases for which no cure is currently available, including Alzheimer's (AD), Huntington's and Parkinson's diseases [1–5]. Despite the differences in the native structures and functions of the amyloid forming proteins, they form similar fibrils irrespective of the protein from which they originate [4,5]. The molecular mechanism of amyloid toxicity is not well understood. The proposed mechanism of amyloid fibril formation involves protein cleavage from the membrane, unfolding and formation of amyloid fibrils [6]. Although fibril plaque formation is associated with biological membranes *in vivo*, the role of membrane surfaces is not well understood. A growing number of recent research contributions suggest the importance of membrane surfaces [4,7–16] and in particular the role of electrostatic interactions between the lipid membrane and amyloid-forming proteins [17–19]. Therefore, the detailed investigation of amyloid fibril formation on the surface of lipid membrane is extremely important and may provide an insight into understanding the mechanism of amyloid fibril formation and toxicity. While biological surfaces are extremely important in protein adsorption and amyloid fibril formation, interpreting the results of heterogeneous and complex systems like plasma membranes is often very difficult. Chemically modified surfaces with well-defined physical properties can be considered as simplified models to study the effect of surfaces on amyloid binding and fibril formation. The study of protein aggregation on surfaces has recently attracted a lot of attention [12,20–24] and grown even more important due to the increased use of inorganic and synthetic surfaces as interfaces in bio- and nano-technology.

It has become evident that surfaces play a crucial role in amyloid fibril formation for many amyloidogenic peptides. The size and shape of amyloid aggregates and fibrils, as well as the kinetics of their formation are affected by the physicochemical nature of the surface. It has been shown that for many amyloid peptides, fibril formation is accelerated significantly by surfaces when compared to fibrillization in solution [24,25]. In addition to catalyzing the rate of fibril formation, the mechanism of fibrillization on surfaces has been shown to be different from that in solution [24].

Although it has been shown that the surfaces play an important role in amyloid fibril formation, electrostatic interaction cannot be easily compared as often experiments presented by different research groups are done at varying experimental conditions, such as pH, temperature, the type of surfaces and the type of peptide used. Protein binding to surfaces at high temperatures cannot be compared to experiments on surfaces conducted at room temperatures [26], nor can different experiments done at different pH [26–31] be compared to elucidate the effect of surfaces. This comparison is also difficult due to the limited type of surfaces used [24] for the same type of amyloid proteins [25,26]. Therefore, more work is required to understand the effect of surface functionality using simple model surfaces before moving to more complex surfaces of lipid bilayer or plasma membrane. Our hypothesis is that the surface charge and hydrophobicity affects the structure, amount and surface coverage of A β deposits and may play an important role when interactions of A β with cell surfaces are considered. To make a clear comparison these surfaces need to be compared under the same conditions in order to elucidate their effect on A β aggregation. Recently Wang et al

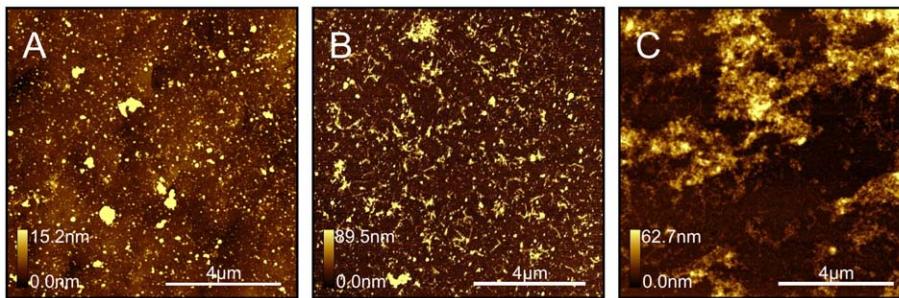


Figure 1. AFM topography images (10×10 μm) of amyloid fibril formation on NH₂- modified surfaces: (A) after 10 minutes, (B) after 6 hours, and (C) after 22 hours incubation at 37°C in HEPES buffer, pH 7.8.
doi:10.1371/journal.pone.0025954.g001

[32,33] reported a systematic molecular dynamics study on A β binding to self-assembled thiol monolayers with four different functional groups.

In our experiments using high resolution atomic force microscopy we studied the interaction of A β (1–42) with three different surfaces: positively charged (NH₂), negatively charged (COOH) and hydrophobic (CH₃) modified surfaces at pH 7.8, at 37°C, in order to determine the effect of these surfaces on amyloid aggregation and fibril formation. In order to understand electrostatic interactions of amyloid aggregates with functionalized surfaces we employed the nonlinear Poisson-Boltzmann equation (PBE) approach [34]. Using this methodology [34–38], it has been demonstrated recently that electrostatic potentials can be successfully calculated for large micromolecules and bioassemblies, which helps to understand the function of these structures. We used the PBE approach to analyze the interactions of amyloid monomers and oligomers with thiol-modified surfaces and compared these to AFM data. To the best of our knowledge, this is a first report where electrostatic interactions of A β peptide and oligomers were compared in similar experimental conditions, combining experimental AFM data and PBE theoretical analysis.

Results and Discussion

Amyloid plaques are formed when proteins which exist in an alpha-helical form, unfold, convert to beta-sheets and form fibrils. Amyloid fibril formation has been studied extensively in solution where the interaction between peptide molecules is mainly considered. According to the proposed hypothesis, interaction between amyloidogenic peptides in solution may result in the formation of various aggregates, such as small oligomers and long fibrils with twisted morphology [3,39] which are formed by attaching monomer units to the end of growing fibrils. However, the structure of protofibrils formed on the surface is different from the twisted morphology of fibrils formed in solution [25,40,41]. The proposed mechanism includes two distinct stages: nucleation and elongation [25,40–44]. According to this model, aggregation of amyloid peptides on surfaces occurs via formation of small oligomeric units. Bidirectional elongation of so-called protofibrils on the surface occurs with the addition of monomers, oligomeric building blocks, or smaller protofibrils. Investigation of these oligomers is of high importance as they recently have been recognized to interact actively with the cell surfaces inducing more toxic effects [45–48] than mature A β fibrils, as it was assumed earlier [49–52]. The size of these oligomeric units depends on the type of the protein and may correspond to monomer, dimer, or small oligomer, or, in some cases, may include up to 20–100 individual peptide molecules [25,40,44].

Time Dependence.

We investigated fibril formation of A β (1–42) peptide on chemically modified surfaces bearing CH₃, COOH, and NH₂ functional groups. A progressive accumulation of A β deposits with time was observed on all surfaces. Figure 1 shows the increase of amyloid fibril formation with time on an NH₂-modified surface. At 10 minutes incubation (Figure 1A) mostly small spherical aggregates and a few small protofibrils were observed on the surface. After 6 hours incubation (Figure 1B), both small spherical aggregates and a growing number of protofibrils were observed. After 22 hours incubation (Figure 1C), fibrils grow in size and form larger clusters of longer fibrils and small oligomers. These amyloid clusters vary from 20–70 nm in height, and fibrils are 500 nm to 2 μm long, 4 nm or 6–8 nm high. Underneath the larger clusters, the surface is covered with small spherical aggregates approximately 2 nm high. These small spherical aggregates were visible on the surfaces at all incubation times. A similar increase in size and amount of aggregation was observed on two other functionalized surfaces, as shown in Figure 1.

Effect of Surfaces

Although all surfaces promoted adsorption of similar smaller building blocks, we observed that the CH₃-modified surface promoted formation of amorphous aggregates, while hydrophilic NH₂- and COOH-modified surfaces showed clusters of small spheres and short protofibrils (Figure 2). Figure 2 shows the AFM topography images of amyloid deposits formed after 22 hours incubation on CH₃-terminated surface (Figure 2A), NH₂-terminated surface (Figure 2B), and COOH-terminated surface (Figure 2C).

Each of these surfaces after 22 hours incubation show large clusters of A β aggregates. The hydrophobic CH₃-terminated surface (Figure 2A) shows amorphous globular clusters of various sizes joined together, but no long separated fibrils were observed on this surface. Both the positively charged NH₂-surface (Figure 2B) and negatively charged COOH-surface (Figure 2C) show clusters of fibril-like structures and uniformly sized globular aggregates. We found that smaller spherical aggregates cover the surface uniformly in between larger clusters (Figure 2 B and C), forming a monolayer which covers the surface completely underneath larger clusters. The density of larger clusters is highest on CH₃-modified surface (Figure 2A) and lowest on NH₂-modified surface (Figure 2B). We performed a statistical analysis of aggregate surface coverage at 22 hours incubation, counting for the second layer of amyloid deposits formed. The CH₃-modified surface is covered by amyloid deposits almost completely (94% surface coverage), whereas the COOH- and NH₂-modified are

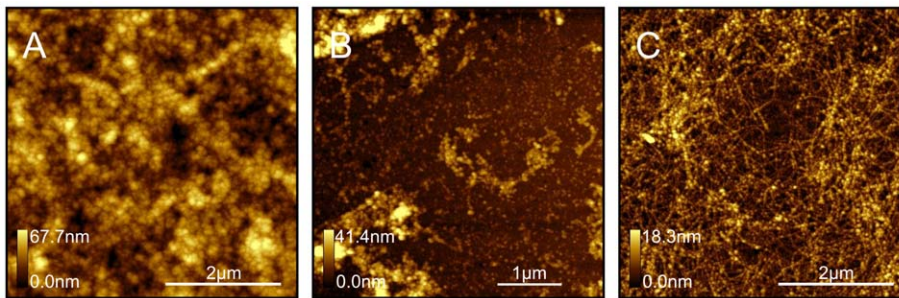


Figure 2. AFM topography images (5×5 μm) of the amyloid fibrils formed on CH₃, NH₂, and COOH -modified surfaces. Aβ peptide solution was incubated for 22 hours at 37°C on: (A) CH₃, (B) NH₂, and (C) COOH-modified surfaces. doi:10.1371/journal.pone.0025954.g002

surfaces covered by amyloid deposits in a less extent, 81.3% and 23.7% respectively (Figure 2).

High resolution images, Figure 3, show clearly that the first monolayer on each surface type is composed of smaller aggregates densely packed together. This monolayer is formed after 1 hour incubation. At 1 hour incubation we also can clearly see few small and separated protofibrils, formed on the top of the monolayer, Figure 3 A, B, C, D, and G. These protofibrils are also composed of spherical aggregates, as shown on Figure 3C, similar in size to the monolayer components.

The shape and size of small oligomers were slightly different for different surfaces. Figure 3C, 3F, and 3I show small scan areas of the monolayer for each surface type. Figure 4 shows results of statistical analysis of size distribution. Both surface area and height plots indicate that the negatively charged COOH-modified surface (Figure 4 C and D) and positively charged NH₂-modified surface (Figure 4 E and F) have smaller aggregates than the CH₃-modified surface (Figure 4 A and B). The Aβ oligomers on the hydrophobic CH₃-modified surface are mostly spherical and less uniform in size, which is revealed by broad

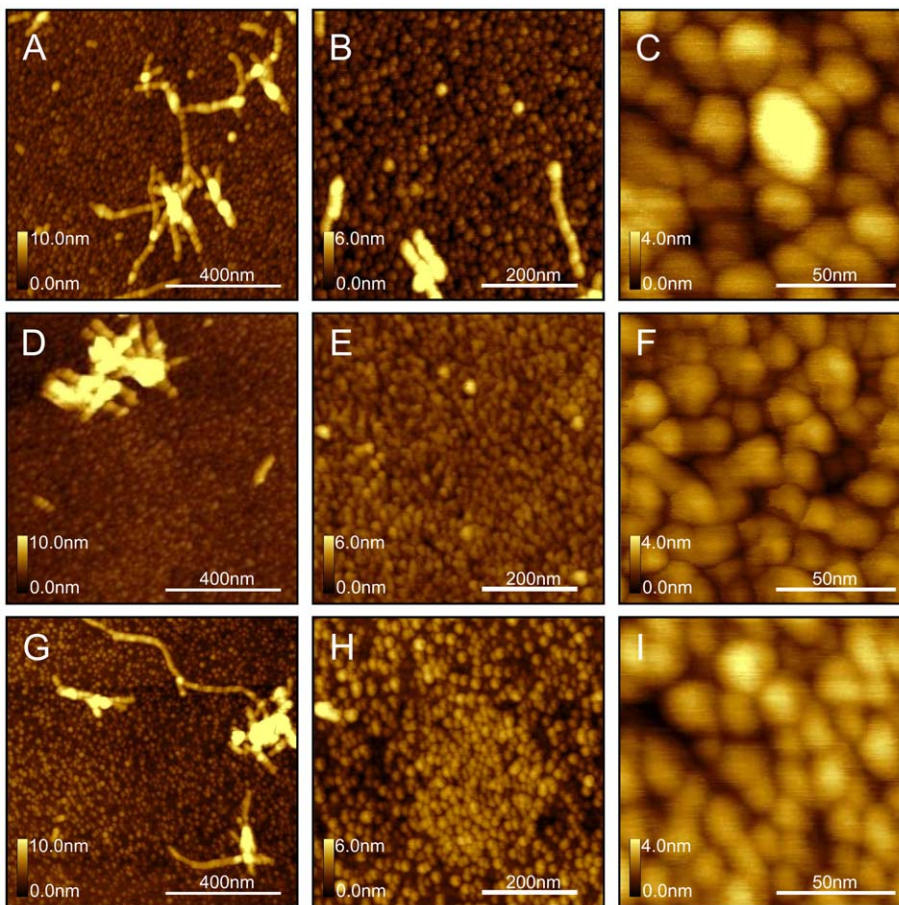


Figure 3. High resolution images of AFM topography of Aβ aggregates formed on modified surfaces: CH₃- (A–C), COOH- (D–F), and NH₂- (G–I) modified surfaces, after incubation with Aβ (1–42) solution (500 μg/ml) for 1 hour at 37°C. doi:10.1371/journal.pone.0025954.g003

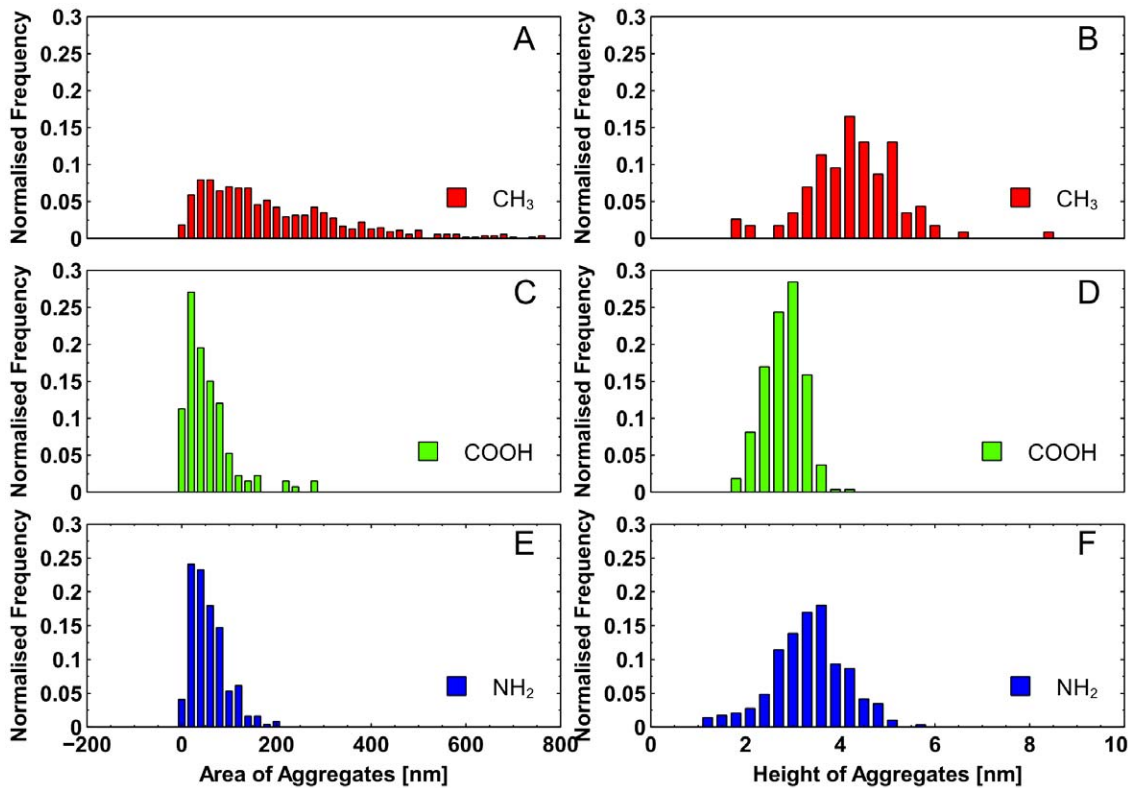


Figure 4. Statistical analysis of A β small aggregates shown in figure 3. Histograms of aggregate unit area size (A, C, E) and height of each aggregate (B, D, F) for each surface type; (Red) CH₃-modified surface; (green) COOH-modified surface; (blue) NH₂-modified surface. doi:10.1371/journal.pone.0025954.g004

height distribution, Figure 4, compared to deposits on charged NH₂ and COOH surfaces.

The presence of small oligomeric units correlates with previously reported oligomer building blocks [39] for A β (1–40). The authors [39–41] observed spherical units of A β (1–40) of varying dimensions immediately following the initiation of fibrillization. It has been shown that stable oligomers of a range of molecular weights of both A β (1–40) and A β (1–42) were isolated from brain and synthetic amyloid material. Size-exclusion chromatography of A β deposits has previously revealed dimeric (9 kDa) and trimeric (13.5 kDa) forms [39,53] whereas incubation of monomeric A β has led to the separation of 4-, 19-, and 46-kDa fragments [54]. Others also reported the presence of oligomer units [53,55,56].

Although we observed small oligomers present on all types of surfaces used, interestingly, these smaller building blocks on the COOH-terminated surface were not spherical, but rather triangular. This may be a result of the interaction with the negatively charged COOH surface. The aggregates making up the monolayer on the NH₂ surfaces were also not completely spherical, but resemble a triangular shape. They appear to be a similar shape to the COOH surface, but more tightly packed together. This indicates that electrostatic interactions with the surfaces may affect the oligomer folding and packing and therefore the shape of the smaller building blocks. Small size triangular shaped oligomers were not observed before, but were proposed by simulations of trimer structures by Paravastu et al. 2008 [57] versus spherical – dimer structures. Wang et al [32] also has shown by molecular dynamics simulations that A β is relatively free to move at the CH₃ surfaces but stick to COOH- and NH₂-surfaces,

which may result in more ordered appearance of A β deposits on charged surfaces, compared to CH₃-surfaces [32].

The electrostatic interactions between the charged surfaces and A β directly influence the structure of formed amyloid deposits and may affect the secondary structure of amyloid in these clusters. These electrostatic interactions can be understood when we consider complex charge distribution in A β peptide and its dependence on secondary structure. There are six negatively charged residues and three positively charged residues in the peptide, yielding a net charge of -3, with isoelectric point of about 5.5 [58]. Figure 5 demonstrates the organization of charge within various peptide secondary structures. For the α -helix structure (Figure 5A), the charge is fairly evenly distributed to prevent a dipole from forming. In the case of a β -sheet (Figure 5B), a strong positively charged region (blue) forms on either side of peptide, and the negatively charged (red) regions are dispersed through the remainder of the peptide. However, when several β -sheets are stacked together (Figure 5C), strong charged regions form within the aggregate creating a quadrupole moment. Therefore, based on this analysis, we expect that α -helical peptides preferentially form on the hydrophobic CH₃ surface, and β -sheet clusters of various sizes on the negatively charged COOH and positively charged NH₂ surfaces.

Our findings at neutral pH correlate with work by McMasters et al [27], where the authors investigated amyloid fibril formation of A β peptide on chemically modified mica bearing positively or negatively charged, or hydrophobic functional groups at pH 11.5. Using reflection-absorption infrared spectroscopy, the authors found that surfaces covered with sulfonic acid, carboxylic acid, alcohol, and trifluoro-terminated thiol monolayers all cause

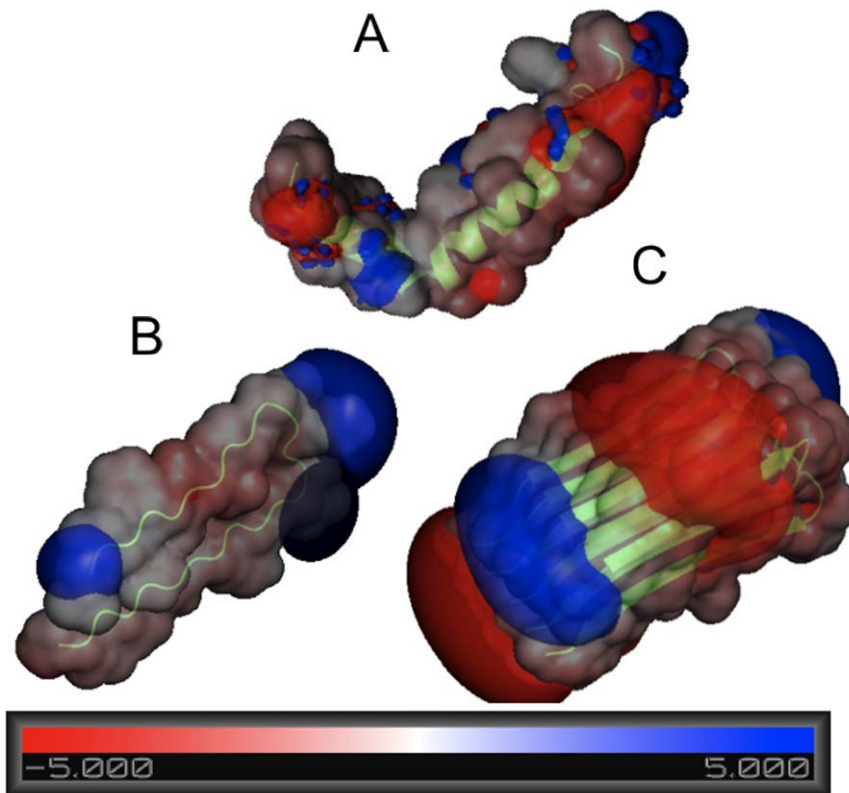


Figure 5. Electrostatic potentials of amyloid monomers and oligomers. The 5kT and -5kT isoelectric potential surfaces are superimposed on the molecular surface. Positive charge is shown in blue, and negative in red. The molecular surface is produced by convolving a 1.4Å sphere (which represents a water molecule) around each peptide. The (A) alpha helix monomer does not have any strongly charged regions, whereas the (B) beta sheet monomer has a strong positively charged end. In comparison, the (C) stack of 5 beta sheets has 4 strongly charged regions, which would greatly contribute to electrostatic interactions with charged surfaces. Images were produced using PyMOL v1.2.
doi:10.1371/journal.pone.0025954.g005

adsorption/deposition of A β (10–35) peptide. Deposits were composed of peptides in beta-sheet, beta-turn, random coil and α -helical conformation. The CF₃ monolayer study revealed that equilibrium is slightly shifted towards an α -helix form. This correlates with our results showing amorphous aggregates, in α -helix form and no fibrils on the CH₃-modified surfaces. Our observation is consistent also with findings by Giacomelli et al [28], who used spectroscopy methods and showed that adsorption of A β (1–40) (at pH 7 and 10, at 25°C) on both hydrophobic Teflon and hydrophilic silica solid surfaces causes conformational changes of the adsorbed peptide, inhibiting polymerization, which occurs in solution during incubation. The conformation of the peptide strongly depends on the hydrophobicity of the surface: hydrophobic interactions promote intramolecular α -helix formation, whereas electrostatic interactions promote intermolecular β -sheet formation. In addition to different structures, we showed that surface-mediated aggregation occurs faster for CH₃-modified and COOH-modified surfaces as compared to NH₂-modified surfaces. This is indicated by larger amyloid surface coverage for CH₃-modified surface and COOH-modified surface shown on Figure 2.

In addition our analysis of electrostatic potential distribution using PBE shows that surface charge distribution is different in A β monomer, dimer or larger oligomers. Oligomers in β -sheet conformations show larger collective polarity, which induces stronger electrostatic interactions with surfaces, as well as preferential ordering on the oligomers on the surfaces. This may be the driving force for more ordered and fibril-like structures observed on charged surfaces, compared to CH₃-modified

surfaces. Electrostatic forces induced by surfaces may also drive the re-distribution of electrostatic potential in monomers near the surfaces and therefore may change the secondary structure of the peptide, thus inducing electrostatically driven amyloid fibril formation.

Incubation of Amyloid Peptide in Solution

We observed that protofibrils formed on surfaces are composed of small spherical units, branched and can grow in any direction by adding the spherical building blocks. Unlike protofibrils formed on surfaces (Figure 3) which are composed of small spheres, fibrils formed in solution (Figure 6) are long, continuous and twisted together into helices, and do not reveal any bead-like structure. This correlates with previously reported data by Blackley et al [40]. The smaller spherical building blocks were not commonly observed in our experiments for fibrils formed in solution (Figure 6), and we rarely observed twisting of protofibrils formed on the surfaces. This suggests that the unfolding of the oligomer units in order to form twisted fibrils is hindered by the surfaces. In solution the peptides have more degrees of freedom (such as rotational, translational, and protein folding), whereas on the surface the degrees of freedom are significantly limited. Additionally, once a peptide is bound to the surface, the peptide has likely found an energy minimum, and therefore requires an energy input to overcome the potential well. Gibbs free energy decreases as a result of the protein absorbing to the surface, and therefore energy must be given to the protein to overcome this decrease [59]. This is consistent with the molecular dynamics simulations data [60,61],

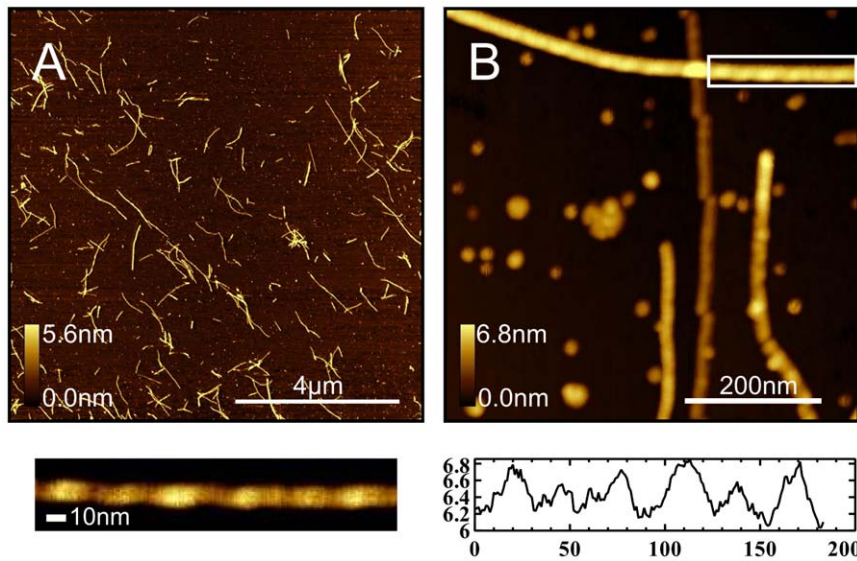


Figure 6. AFM topography images of A β (1–42) incubated in solution (500 μ g/mL concentration) at 37°C for 22 hours. After incubation, 10 μ L of solution was deposited onto cleaved mica for 5 minutes, followed by rinsing with nanopure water and drying with a gentle nitrogen stream. A 10 \times 10 μ m scan area (A) of the surface shows many fibrils ranging from 0.1 – 4 μ m. (B) High resolution image (500 \times 500nm) demonstrates that fibrils reveal twisted morphologies, characteristic of formed in solution; (below, left) expanded view of region enclosed by white box in (B) with optimized z-scale; (below, right) height profile along fibril axis clearly demonstrating maxima and minima which is characteristic of the twisted morphology.

doi:10.1371/journal.pone.0025954.g006

which indicate that for larger oligomer sizes or long chain lengths, it is very unlikely for the chain to fold into ordered β -sheet structures. It is much more common for the chains to fold into amorphous aggregates which are in dynamic equilibrium.

Conclusions

We investigated the interaction of A β (1–42) peptide with three different chemically modified surfaces and compared the effect of these surfaces at the same physiologically relevant conditions. We found that due to the complex dipole distribution amyloid oligomers bind to all surface types investigated (-CH₃, -COOH, and -NH₂) although the size and shape of these amyloid deposits depend on surface properties. Hydrophilic surfaces show protofibrils coexisting with spherical oligomer aggregates, while hydrophobic CH₃-modified surfaces cause formation of amorphous spherical aggregates. The surface charge and hydrophobicity define both the structure of the fibril aggregates formed on the surfaces and kinetics of their accumulation. In addition our analysis of electrostatic potential distribution using PBE shows that surface charge distribution changes depending on the secondary structure of the peptide and may play an important role in electrostatically driven amyloid fibril formation on surfaces.

Materials and Methods

Chemicals and Sample Preparation

Decanethiol, 3-mercaptoethanol, APTES (3-Aminopropyltriethoxysilane) and HEPES buffer were purchased from Aldrich Chemical Co. HPLC grade ethanol was purchased from Sigma. All chemicals were used as received. Water used for sample preparation was purified (distilled de-ionized, millipore water).

Substrate Preparation

Atomically flat gold on mica surfaces were purchased from Agilent Technologies, Inc. (Santa Clara, CA). These gold surfaces

were affixed to clean glass cover slips using Epo-Tek 377 glue from Epo-Tek, Inc. (Billerica, MA), which was cured at 150°C for 1 hour. The gold glued to the glass was peeled from the mica, revealing the atomically flat gold surface. The gold surfaces were further modified by incubating in an appropriate 5 mM thiol solution in ethanol for 48 hours. Prepared mica-gold substrates were modified with decanethiol and 3-mercaptoethanol, and pure glass substrates were modified with APTES.

Amyloid Peptide Preparation and Incubation

A β (1–42) was purchased freeze-dried in 0.5 mg vials from rPeptide (Atlanta, GA). These amyloid samples were pretreated according to the Fezoui et al. (2000) procedure [62] to ensure monomeric solution. After this each 0.5 mg aliquot was dissolved in 1 mL of pH 7.8 50 mM HEPES buffer. Small amount of the protein solution (50 μ L aliquots) were immediately placed on modified surface and were incubated at 37°C in liquid cell. After defined period of time (from 10 min to 22 hours) samples were rinsed with millipore DI water, dried with gentle stream of nitrogen, and kept in a desiccator prior to imaging.

AFM Imaging and Analysis

Imaging was done in intermittent contact mode on a JPK Nanowizard II atomic force microscope (AFM) recorded with AC mode, and on an Agilent AFM/SPM-5500 AFM using MAC mode imaging. Images were obtained with Nanoworld NCH tips, with a resonant frequency of 338 kHz and 42 N/m spring constant in air or Agilent MAC mode cantilevers, with a resonant frequency of 75 kHz and a spring constant of 2.8 N/m in air.

Statistical analysis was done with the program called CellProfiler. The shape of each amyloid aggregate was measured using image recognition. The purpose of the program is to count the number of spherical aggregates (or cells) in an image. Using this program we determined the size and shape of the aggregates. The

total number of measurements used for analysis is: 133 for CH₃, 543 for COOH, and 245 for NH₂ surfaces.

Electrostatic Modeling

Electrostatic potentials of A β monomers in β -sheet and α -helix conformations, and amyloid oligomers were obtained by solving the Adaptive Poisson-Boltzmann Solver (APBS v1.2.1b) [35,63] implementation for PyMol v1.2. Briefly, the APBS method uses the finite element method to numerically solve the nonlinear Poisson-Boltzmann equation, representing the electrostatic interactions between molecules in aqueous environments [34]. We constructed surface potential profiles for A β monomers in β -sheet and α -helix conformations and amyloid pentamers based on crystalline structure obtained from protein data bank [64,65].

The electrostatic interaction energies are calculated for each voxel within a defined volume. In our calculations the solvent

dielectric constant was 80, and the protein dielectric was approximated as 2.0. The isoelectric potential of 5kT and -5kT was mapped onto the A- β monomers and beta sheet oligomer. The monomers and oligomers are displayed by convolving a 1.4Å sphere representing the approximate solvent size.

Acknowledgments

The authors acknowledge technical support from Dr. Song Xu (Agilent Technologies) and Dr. Christian Löbbe, Dr. Sid Ragona (JPK Instruments).

Author Contributions

Conceived and designed the experiments: ZL BM. Performed the experiments: BM JS. Analyzed the data: BM ED SA. Contributed reagents/materials/analysis tools: ZL. Wrote the paper: BM JS ED SA ZL.

References

- Lashuel HA, Lai Z, Kelly JW (1998) Characterization of the Transthyretin Acid Denaturation Pathway by Analytical Ultracentrifugation: Implications for wild type, V30M and L55P Amyloid Fibril Formation. *Biochem* 37: 17851–17864.
- Lansbury P, Rochet J (2000) Amyloid fibrillogenesis: themes and variations. *Curr Opin Struct Biol* 10: 60–68.
- Chiti F, Dobson CM (2006) Protein misfolding, functional amyloid, and human disease. *Annu Rev Biochem* 75: 333–366.
- Dobson CM (2001) The Structural Basis of Protein Folding and its Links with Human Disease. *Phil Trans R Soc Lond B* 356: 133–145.
- Johansson J (2003) Molecular determinants for amyloid fibril formation: lessons from lung surfactant protein C. *Swiss Med Wkly* 133: 275–282.
- Carrell R, Gooptu B (1998) Conformational Changes and Disease - Serpins, Prions and Alzheimer's. *Curr Opin Struct Biol* 8: 799–809.
- Lin HAI, Bhatia R, Lal R (2001) Amyloid Beta Protein Forms Ion Channels: Implications for Alzheimer's Disease Pathophysiology. *FASEB J* 13: 2433–2444.
- Quist A, Doudevski I, Lin H, Azimova R, Ng D, et al. (2005) Amyloid Ion Channels: A Common Structural Link for Protein-Misfolding Disease. *Proc Natl Acad Sci USA* 102: 10427–10432.
- Kayed R, Sokolov Y, Edmonds B, McIntire TM, Milton SC, et al. (2004) Permeabilization of Lipid Bilayers is a Common Conformation-Dependent Activity of Soluble Amyloid Oligomers in Protein Misfolding Diseases. *J Biol Chem* 279: 46363–46366.
- Ambroggio EE, Kim DH, Separovic F, Barrow CJ, Barnham KJ, et al. (2005) Surface Behavior and Lipid Interaction of Alzheimer Beta-Amyloid Peptide 1-42: A Membrane-Disrupting Peptide. *Biophys J* 88: 2706–2713.
- Cordy JM, Hooper NM, Turner AJ (2006) The Involvement of Lipid Rafts in Alzheimer's Disease. *Mol Membr Biol* 23: 111–122.
- Sharp JS, Jones RAL, Forrest JA (2002) Surface Denaturation and Amyloid Fibril Formation of Insulin at Model Lipid-Water Interfaces. *Biochem* 41: 15810–15819.
- Ege C, Majewski J, Wu G, Kjaer K, Lee KY (2005) Templating Effect of Lipid Membranes on Alzheimer's Amyloid. *Chemphyschem* 6: 226–229.
- Yip CM, Elton EA, Darable AA, Morrison MR, McLaurin J (2001) Cholesterol, A Modulator of Membrane-Associated A β -Fibrillogenesis and Neurotoxicity. *J Mol Biol* 311: 723–734.
- Choucair A, Chakrapani M, Chakravarthy B, Katsaras J, Johnston L (2007) Preferential Accumulation of Abeta(1-42) on Gel Phase Domains of Lipid Bilayers: An AFM and Fluorescence Study. *Biochim Biophys Acta Biomembr* 1768: 146–154.
- Terzi E, Hölzemann G, Seelig J (1995) Self-Association of Beta-Amyloid Peptide (1-40) in Solution and Binding to Lipid Membranes. *J Mol Biol* 252: 633–642.
- Choo-Smith LP, Rodriguez W, Glabe C, Surewicz W (1997) Acceleration of Amyloid Fibril Formation By Specific Binding of β -Amyloid Peptide (1–40) to Ganglioside-Containing Membrane Vesicles. *J Biol Chem* 272: 22987–22990.
- Kakio A, Nishimoto S, Yanagisawa K, Kozutsumi Y, Matsuzaki K (2002) Interactions of Amyloid Beta-Protein with Various Gangliosides in Raft-Like Membranes: Importance of GM1 Ganglioside-Bound Form as an Endogenous Seed for Alzheimer Amyloid. *Biochem* 41: 7385–7390.
- Yanagisawa K, Odaka ASuzuki N, Ihara Y (1995) GM1 Ganglioside-Bound Amyloid β -Protein (A β): A Possible Form of Preamyloid in Alzheimer's Disease. *Nat Med* 1: 1062–1066.
- Nayak A, Dutta AK, Belfort G (2008) Surface-Enhanced Nucleation of Insulin Amyloid Fibrillation. *Biochem Biophys Res Comm* 369: 303–307.
- Sethuraman A, Belfort G (2005) Protein Structural Perturbation and Aggregation on Homogeneous Surfaces. *Biophys J* 88: 1322–1333.
- Yang H, Fung S, Pritzker M, Chen P (2007) Surface-Assisted Assembly of an Ionic-Complementary Peptide: Controllable Growth of Nanofibers. *J Am Chem Soc* 129: 12200–12210.
- Sigal GB, Mrksich M, Whitesides GM (1998) Effects of Surface Wettability on the Adsorption of Proteins and Detergents. *J Am Chem Soc* 120: 3464–3473.
- Powers ET, Kelly JW (2001) Medium-Dependent Self-Assembly of an Amphiphilic Peptide: Direct Observation of Peptide Phase Domains at the Air-Water Interface. *J Am Chem Soc* 123: 775–776.
- Zhu M, Souillac PO, Ionescu-Zanetti C, Carter SA, Fink AL (2002) Surface-Catalyzed Amyloid Fibril Formation. *J Biol Chem* 277: 50914–50922.
- Hammarström P, Ali MM, Mishra R, Svensson SA (2008) Catalytic Surface for Amyloid Fibril Formation. *J Phys. Conf Ser* 100: 052039.
- McMasters MJ, Hammer RP, McCarley RL (2005) Surface-Induced Aggregation of Beta Amyloid Peptide by ω -Substituted Alkanethiol Monolayers Supported on Gold. *Langmuir* 21: 4464–4470.
- Giacomelli CE, Norde W (2005) Conformational Changes of the Amyloid β -Peptide (1-40) Adsorbed on Solid Surfaces. *Macromol Biosci* 5: 401–407.
- Uversky VN, Li J, Fink AL (2001) Evidence for a Partially-Folded Intermediate in Alpha-Synuclein Fibril Formation. *J Biol Chem* 276: 10737–10744.
- Qin Z, Hu D, Zhu M, Fink AL (2007) Structural Characterization of the Partially Folded Intermediates of an Immunoglobulin Light Chain Leading to Amyloid Fibrillation and Amorphous Aggregation. *Biochemistry* 46: 3521–3531.
- Yokoyama K, Welchons DR (2007) The Conjugation of Amyloid Beta Protein on the Gold Colloidal Nanoparticles' Surfaces. *Nanotechnology* 18: 105101–105107.
- Wang Q, Zhao J, Yu Z, Zhao C, Li L, et al. (2010) Alzheimer A- β 1-42 Monomer Adsorbed on the Self-Assembled Monolayers. *Langmuir* 26: 12722–12732.
- Wang Q, Zhao C, Zhao J, Wang J, Yang JC, et al. (2010) Comparative Molecular Dynamics Study of A β Adsorption on the Self-Assembled Monolayers. *Langmuir* 26: 3308–3316.
- Baker NA, Sept D, Joseph S, Holst MJ, McCammon JA (2001) Electrostatics of Nanosystems: Application to Microtubules and the Ribosome. *Proc Natl Acad Sci USA* 98: 10037–10041.
- Sharp KA (1994) Electrostatic Interactions in Macromolecules. *Curr Opin Struct Biol* 4: 234–239.
- Guo T, Gong LC, Sui SF (2010) An Electrostatically Preferred Lateral Orientation of SNARE Complex Suggests Novel Mechanisms for Driving Membrane Fusion. *PLoS ONE* 5: e8900.
- Dolinsky TJ, Nielsen JE, McCammon JA, Baker NA (2004) PDB2PQR: An Automated Pipeline for the Setup of Poisson-Boltzmann Electrostatics Calculations. *Nucleic Acids Res* 32: 665–667.
- Cohen FS, Melikyan GB (2004) The Energetics of Membrane Fusion from Binding, Through Hemifusion, Pore Formation, and Pore Enlargement. *J Membr Biol* 199: 1–14.
- Blackley HKL, Patel N, Davies MC, Roberts CJ, Tendler SJB, et al. (1999) Morphological Development of β (1-40) Amyloid Fibrils. *Exp Neurol* 158: 437–443.
- Blackley HKL, Sanders GHW, Davies MC, Roberts CJ, Tendler SJB, et al. (2000) In-situ Atomic Force Microscopy Study of β -Amyloid Fibrillation. *J Mol Biol* 298: 833–840.
- Rocha S, Krastev R, Thünemann AF, Pereira MC, Möhwald H, et al. (2005) Adsorption of Amyloid β -Peptide at Polymer Surfaces: A Neutron Reflectivity Study. *ChemPhysChem* 6: 2527–2534.
- Kowalewski T, Holtzman DM (1999) *In situ* Atomic Force Microscopy Study of Alzheimer's β -Amyloid Peptide on Different Substrates: New Insights into Mechanism of β -Sheet Formation. *Proc Natl Acad Sci USA* 96: 3688–3693.
- Jarrett JT, Berger EP, Lansbury PT (1993) The Carboxy Terminus of the Beta Amyloid Protein is Critical for the Seeding of Amyloid Formation: Implications of the Pathogenesis of Alzheimer's Disease. *Biochemistry* 32: 4693–4697.

44. Lomakin A, Chung DS, Benedek GB, Kirschner DA, Teplow DB (1996) On the Nucleation and Growth of Amyloid β -Protein Fibrils: Detection of Nuclei and Quantitation of Rate Constants. *Proc Natl Acad Sci USA* 93: 1125–1129.
45. Goldberg MS, Lansbury PT (2000) Is There a Cause-and-Effect Relationship Between Alpha-Synuclein Fibrillization and Parkinson's Disease? *Nat Cell Biol* 2: E115–E119.
46. Stefani M (2007) Generic Cell Dysfunction in Neurodegenerative Disorders: Role of Surfaces in Early Protein Misfolding, Aggregation, and Aggregate Cytotoxicity. *Neuroscientist* 13: 519–531.
47. Buxbaum J, Gallo G (1999) Nonamyloidotic Monoclonal Immunoglobulin Deposition Disease. Light-Chain, Heavy-Chain, and Light- and Heavy-Chain Deposition Diseases. *Hematol Oncol Clin North Am* 13: 1235–1248.
48. Lambert MP, Barlow AK, Chromy BA, Edwards C, Freed R, et al. (1998) Diffusible, Nonfibrillar Ligands Derived from Abeta1-42 are Potent Central Nervous System Neurotoxins. *Proc Natl Acad Sci USA* 95: 6448–6453.
49. Howlett DR, Jennings KH, Lee DCC, Clark MSG, Brown F, et al. (1995) Aggregation State and Neurotoxic Properties of Alzheimer Beta-Amyloid Peptide. *Neurodegener* 4: 23–32.
50. Pike CJ, Walencewicz AJ, Glabe CG, Cotman CW (1991) In vitro Aging of β -Amyloid Protein Causes Peptide Aggregation and Neurotoxicity. *Brain Res* 563: 311–314.
51. Pike CJ, Burdick D, Walencewicz AJ, Glabe CG, Cotman CW (1993) Neurodegeneration Induced by β - Amyloid Peptides *in vitro*: The Role of Peptide Assembly State. *J Neurosci* 13: 1676–1687.
52. Seilheimer B, Bohrmann B, Bondolfi L, Muller F, Stuber D, et al. (1997) The Toxicity of the Alzheimer's Beta-Amyloid Peptide Correlates with a Distinct Fiber Morphology. *J Struct Biol* 119: 59–71.
53. Roher AE, Chaney MO, Kuo YM, Webster SD, Stine WB, et al. (1996) Morphology and Toxicity of $A\beta$ -(1-42) Dimer Derived from Neuritic and Vascular Amyloid Deposits of Alzheimer's Disease. *J Biol Chem* 271: 20631–20635.
54. Dyrks T, Dyrks E, Masters C, Beyreuther K (1993) Amyloidogenicity of Rodent and Human Beta A4 Sequences. *FEBS Lett* 324: 231–236.
55. Kuo Y, Emmerling ER, Vigo-Pelfrey C, Kasunic TC, Kirkpatrick JB, et al. (1996) Water-Soluble $A\beta$ (N-40, N-42) Oligomers in Normal and Alzheimer Disease Brains. *J Biol Chem* 271: 4077–4081.
56. Levine H (1995) Soluble Multimeric Alzheimer Beta (1-40) Pre-Amyloid Complexes in Dilute Solution. *Neurobiol Aging* 16: 755–764.
57. Paravastu AK, Leapman RD, Yau WM, Tycko R (2008) Molecular Structural Bias for Polymorphism in Alzheimer's β -Amyloid Fibrils. *Proc Natl Acad Sci USA* 105: 18349–18354.
58. Rauk A (2009) The Chemistry of Alzheimer's Disease. *Chem Soc Rev* 38: 2698–2715.
59. Latour RA, Rini CJ (2002) Theoretical Analysis of Adsorption Thermodynamics for Hydrophobic Peptide Residues on SAM Surfaces of Varying Functionality. *J Biomed Mater Res* 60: 564–577.
60. Boucher G, Mousseau N, Derreumaux P (2006) Aggregating the Amyloid $A\beta_{11-25}$ Peptide into a Four-Stranded β -Sheet Structure. *Proteins: Struct, Funct Bioinf* 65: 877–888.
61. Melquiond A, Gelly JC, Mousseau N, Derreumaux P (2007) Probing Amyloid Fibril Formation of the NFGAIL Peptide by Computer Simulations. *J. Chem Phys* 126: 25101–25106.
62. Fezoui Y, Hartley D, Harper J, Khurana R, Walsh D, et al. (2000) An Improved Method of Preparing the Amyloid P-Protein for Fibrillogenesis and Neurotoxicity Experiments. *Amyloid: Int J Exp Clin Invest* 7: 166–178.
63. Sharp KA, Honig B (1990) Calculating Total Electrostatic Energies with Nonlinear Poisson-Boltzmann Equation. *J Phys Chem* 94: 7684–7692.
64. Crescenzi O, Tomaselli S, Guerrini R, Salvadori S, D'Ursi AM, et al. (2002) Solution Structure of the Alzheimer's Disease Amyloid Beta-Peptide (1-42). *Eur J Biochem* 269: 5642–5648.
65. Luhrs T, Ritter C, Adrian M, Riek-Loher D, Bohrmann B, et al. (2005) 3D Structure of Alzheimer's Amyloid- β (1-42) Fibrils. *Proc Natl Acad Sci USA* 102: 17342–17347.